

RESEARCH ARTICLE

Physiological and metabolomic consequences of reduced expression of the *Drosophila brummer* triglyceride Lipase

Nestor O. Nazario-Yepiz, Jaime Fernández Sobaberas[‡], Roberta Lyman, Marion R. Campbell, III, Vijay Shankar, Robert R. H. Anholt, Trudy F. C. Mackay[‡]*

Department of Biochemistry and Genetics and Center for Human Genetics, Clemson University, Greenwood, South Carolina, United States of America

‡ Current address: Centre for Organismal Studies, Heidelberg University, Heidelberg, Germany

* tmackay@clemson.edu



OPEN ACCESS

Citation: Nazario-Yepiz NO, Fernández Sobaberas J, Lyman R, Campbell MR, III, Shankar V, Anholt RRH, et al. (2021) Physiological and metabolomic consequences of reduced expression of the *Drosophila brummer* triglyceride Lipase. PLoS ONE 16(9): e0255198. <https://doi.org/10.1371/journal.pone.0255198>

Editor: Girish C. Melkani, UAB School of Medicine, UNITED STATES

Received: July 8, 2021

Accepted: September 7, 2021

Published: September 21, 2021

Copyright: © 2021 Nazario-Yepiz et al. This is an open access article distributed under the terms of the [Creative Commons Attribution License](https://creativecommons.org/licenses/by/4.0/), which permits unrestricted use, distribution, and reproduction in any medium, provided the original author and source are credited.

Data Availability Statement: All relevant data are within the manuscript and its [Supporting Information](#) files.

Funding: This work was funded by the National Institutes of Health grant R01 GM128974 (<https://www.nigms.nih.gov/>) to T. F. C. M. and R. R. R.H. The funders had no role in study design, data collection and analysis, decision to publish, or preparation of the manuscript.

Abstract

Disruption of lipolysis has widespread effects on intermediary metabolism and organismal phenotypes. Defects in lipolysis can be modeled in *Drosophila melanogaster* through genetic manipulations of *brummer* (*bmm*), which encodes a triglyceride lipase orthologous to mammalian Adipose Triglyceride Lipase. RNAi-mediated knock-down of *bmm* in all tissues or metabolic specific tissues results in reduced locomotor activity, altered sleep patterns and reduced lifespan. Metabolomic analysis on flies in which *bmm* is downregulated reveals a marked reduction in medium chain fatty acids, long chain saturated fatty acids and long chain monounsaturated and polyunsaturated fatty acids, and an increase in diacylglycerol levels. Elevated carbohydrate metabolites and tricarboxylic acid intermediates indicate that impairment of fatty acid mobilization as an energy source may result in upregulation of compensatory carbohydrate catabolism. *bmm* downregulation also results in elevated levels of serotonin and dopamine neurotransmitters, possibly accounting for the impairment of locomotor activity and sleep patterns. Physiological phenotypes and metabolomic changes upon reduction of *bmm* expression show extensive sexual dimorphism. Altered metabolic states in the *Drosophila* model are relevant for understanding human metabolic disorders, since pathways of intermediary metabolism are conserved across phyla.

Introduction

Metabolic syndrome and metabolic diseases impact a large proportion of the world population: a global analysis of 195 countries showed that 604 million adults and 108 million children had obesity in 2015 [1,2]. Although diets with poor ratios of nutrients coupled with a reduction of physical activity contribute to metabolic diseases, genetic risk alleles in different populations are also major contributors [3]. Obesity can impair cognition and increase the risk for psychiatric conditions [4], but the link between obesity and brain function is unclear [5].

Drosophila provides a powerful model system for comprehensive analyses of physiological, behavioral and metabolomic consequences of disruption of intermediary metabolism through

Competing interests: The authors have declared that no competing interests exist.

selective tissue-specific disruption of target genes under controlled dietary conditions [6–9]. Comprehensive studies in *Drosophila* are further facilitated through the public availability of a wide array of genetic resources that can facilitate in-depth systems genetic studies of metabolic regulation [10–15]. *Drosophila* has organ systems analogous to those of mammals that control the uptake, storage and metabolism of nutrients [16]. Digestion and absorption of lipids occur in the midgut, from where lipids are transported by lipoproteins through the hemolymph to other organs [17]. Following feeding, the fat body stores lipids taken up from the hemolymph as triacylglycerides (TAGs) and cholesterol esters. This organ performs lipogenesis by converting carbohydrates via the glycolytic pathway into TAGs and lipolysis to release fatty acids from TAGs when energy is needed. Oenocytes, specialized hepatocyte-homologous cells in *Drosophila*, are required with the fat body for regulation of lipid mobilization [18].

Lipids in the fat body are accumulated in lipid droplets. Their release is controlled by adipokinetic hormone (Akh), the functional counterpart of glucagon in humans, via a G protein-coupled Akh receptor (Akh-R) pathway [19,20]. Akh-R signaling uses a canonical cAMP/PKA signal transduction pathway to regulate the phosphorylation of Perlipin1, which allows access to TAG lipases in lipid droplets [21]. Activation of Akh-R signaling also regulates the expression of the triglyceride lipase *brummer* (*bmm*) [9,22].

bmm is the ortholog of the human *PNPLA2* gene that encodes Adipose Triglyceride Lipase (ATGL), the major mammalian TAG lipase. ATGL hydrolyzes TAGs at the sn-1 and sn-2 positions to release fatty acids for catabolism. Homozygous *bmm* null alleles exhibit embryonic lethality, but some “escapers” reach the adult stage and present excessive fat storage [23]. Humans with mutations in the *bmm* ortholog *PNPLA2* have neutral lipid storage disease with myopathy (NLSDM), characterized by abnormal accumulation of fat in different tissues [24]. Regulation of the balance between lipid storage and breakdown through *bmm* is sexually dimorphic and under neural control [25]. Defects in lipid metabolism are associated with various neurodegenerative diseases in *Drosophila* [26], but little is known about the behavioral phenotypes and physiological effects of *bmm* downregulation.

Here, we show that RNAi-mediated suppression of *bmm* results in impaired locomotion and altered sleep patterns. Metabolomic analysis shows that these effects are accompanied by shifts in intermediary metabolism and changes in levels of neurotransmitters in the brain.

Results

RNAi-mediated reduction in *bmm* expression

We used targeted RNA interference to reduce the expression of *bmm*. We employed in all experiments only one copy of the *Gal4* driver and *UAS-bmm-RNAi* to generate hypomorphic effects. First, we analyzed *bmm* transcript levels with ubiquitous expression of *bmm-RNAi* in adult flies using RT-qPCR. We used two different *UAS-bmm-RNAi* constructs, *bmm-RNAi*^{V37877} and *bmm-RNAi*^{V37880}. For both *Ubi > bmm-RNAi* flies, levels of *bmm* transcripts were significantly lower compared to their controls for both sexes, but the effect of *Ubi > bmm-RNAi*^{V37877} was more pronounced than the effect of *Ubi > bmm-RNAi*^{V37880}. The reduction of *bmm* transcripts was greater in males than in females for both genotypes (Fig 1A and S1 Table). Both RNAi constructs affected the same phenotypes, described below, but the effects were quantitatively different due to differences in the magnitude of *bmm* knockdown. For example, *Ubi > bmm-RNAi*^{V37877} males, which showed the greatest reduction in *bmm* transcript, exhibited a phenotype of spread wings, which was not observed in other knock-down genotypes (Fig 1B).

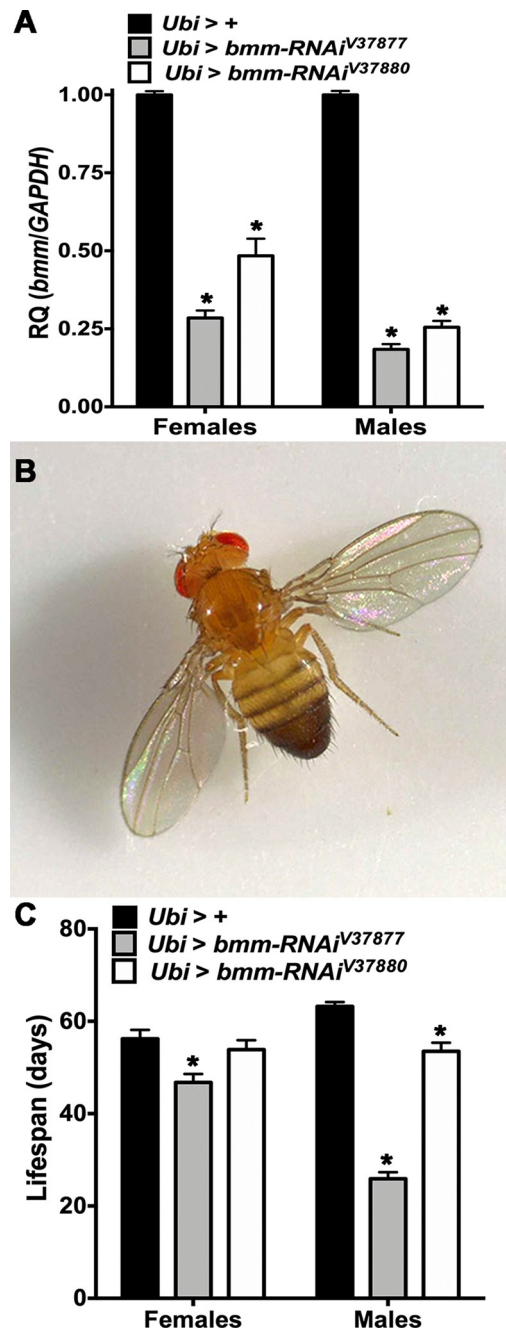


Fig 1. RT-qPCR and lifespan of *Ubi* > *bmm-RNAi* flies. Offspring of *Ubi-Gal4* mated with GD control (*Ubi* > +) or *UAS-bmm-RNAi* flies (*Ubi* > *bmm-RNAi*^{V37877} and *Ubi* > *bmm-RNAi*^{V37880}) were used for the assays. Asterisks indicate significant differences at $p < 0.05$ compared with the appropriate female or male control, following Tukey's correction for multiple tests. (a) RT-qPCR ($n = 9$ for females and males of each genotype), relative quantification (RQ) was done using the $2^{-\Delta\Delta C_t}$ method, and *GAPDH* was used as an internal standard. (b) Spread wings phenotype in males of *Ubi* > *bmm-RNAi*^{V37877} (100%, $n = 100$). (c) Average lifespan for *Ubi* > + ($n = 132$ for females and 118 for males), *Ubi* > *bmm-RNAi*^{V37877} ($n = 136$ for females and 134 for males) and *Ubi* > *bmm-RNAi*^{V37880} ($n = 137$ for females and 132 for males). Error bars are standard errors of the mean (SEM). ANOVA tests are reported in [S1 Table](#).

<https://doi.org/10.1371/journal.pone.0255198.g001>

***Ubi* > *bmm*-RNAi flies have reduced lifespan**

To corroborate previously reported effects on lifespan of *bmm* mutant escapers [23], we measured lifespan of *Ubi* > *bmm*-RNAi flies under standard culture conditions. Females of *Ubi* > *bmm*-RNAi^{V37877} and males of both *Ubi* > *bmm*-RNAi lines had reduced lifespan in a sex biased manner (Fig 1C and S1 Table). Moreover, penetrance of this phenotype matched perfectly with the titration of *bmm* transcript level of *Ubi* > *bmm*-RNAi flies. The level of *bmm* transcript of our allelic series ranged from high hypomorphic to low hypomorphic as follows: *Ubi* > *bmm*-RNAi^{V37877} males, *Ubi* > *bmm*-RNAi^{V37880} males, *Ubi* > *bmm*-RNAi^{V37877} females and *Ubi* > *bmm*-RNAi^{V37880} females.

***bmm* downregulation reduces locomotor activity**

We used locomotor activity as a phenotypic read-out for impaired energy metabolism as a consequence of reduced triglyceride access due to *bmm* down regulation. We recorded continuous activity of *Ubi* > *bmm*-RNAi flies for one week using the Drosophila Activity Monitor (DAM) system. The 24h locomotor activity was significantly lower in *Ubi* > *bmm*-RNAi^{V37877} males than control males (Fig 2A). Locomotor activity was reduced both during the daytime and the nighttime (Fig 2B), which is apparent from their average activity profiles (see also Fig 2C and S2 Table).

To verify that the effect on locomotor activity in *Ubi* > *bmm*-RNAi^{V37877} males was not due to the spread-wings phenotype, we also recorded their activity after removing their wings. Although wing removal affected locomotor activity in all flies, the total 24h locomotor activity (Fig 2D) and activity during the daytime (Fig 2E) were still lowest in these males (see also Fig 2F and S2 Table). Total activity and daytime activity were also reduced in females of both *Ubi* > *bmm*-RNAi flies without wings compared to controls.

To assess the effect of starvation on locomotor activity when *bmm* expression is reduced, we recorded locomotor activity in DAM tubes containing 1% agar for 3 days. Flies that died during the assay were discarded from further analyses. All flies were more active under starvation conditions, but total 24h locomotor activity (Fig 2G) and daytime activity (Fig 2H) was still reduced in *Ubi* > *bmm*-RNAi^{V37877} males and *Ubi* > *bmm*-RNAi^{V37880} females (see also Fig 2I and S2 Table) compared with control flies. Interestingly, *Ubi* > *bmm*-RNAi^{V37880} males were more active under food deprivation during the whole day and during the daytime (Fig 2G and 2H).

***bmm* downregulation results in altered sleep patterns**

We next assessed whether impaired energy metabolism would affect sleep patterns in addition to locomotor activity (see ANOVA tests in S3 Table). We evaluated sleep behavior of *Ubi* > *bmm*-RNAi flies and found that *Ubi* > *bmm*-RNAi^{V37880} females had fewer sleep bouts than control flies (Fig 3A). Conversely, males of both *bmm*-RNAi lines had more sleep bouts than control flies, but the bouts were shorter (Fig 3B). *Ubi* > *bmm*-RNAi^{V37877} males slept more during the daytime, but *Ubi* > *bmm*-RNAi^{V37880} males slept less (Fig 3C). In contrast, *Ubi* > *bmm*-RNAi^{V37877} females had normal sleep bouts but rested more during the daytime. Sleep bouts were not affected in flies without wings (Fig 3D), but *Ubi* > *bmm*-RNAi^{V37877} males had longer sleep bouts (Fig 3E) and slept more during the daytime and nighttime (Fig 3F). Also, females with ubiquitous expression of both *bmm*-RNAi lines napped more during the daytime.

Under starvation conditions all flies had less sleep bouts than under normal feeding (Fig 3A and 3G). Starved *Ubi* > *bmm*-RNAi males of both lines had more sleep bouts (Fig 3G) and the bouts were shorter (Fig 3H) than starved control males. Interestingly, starved *Ubi* > *bmm*-

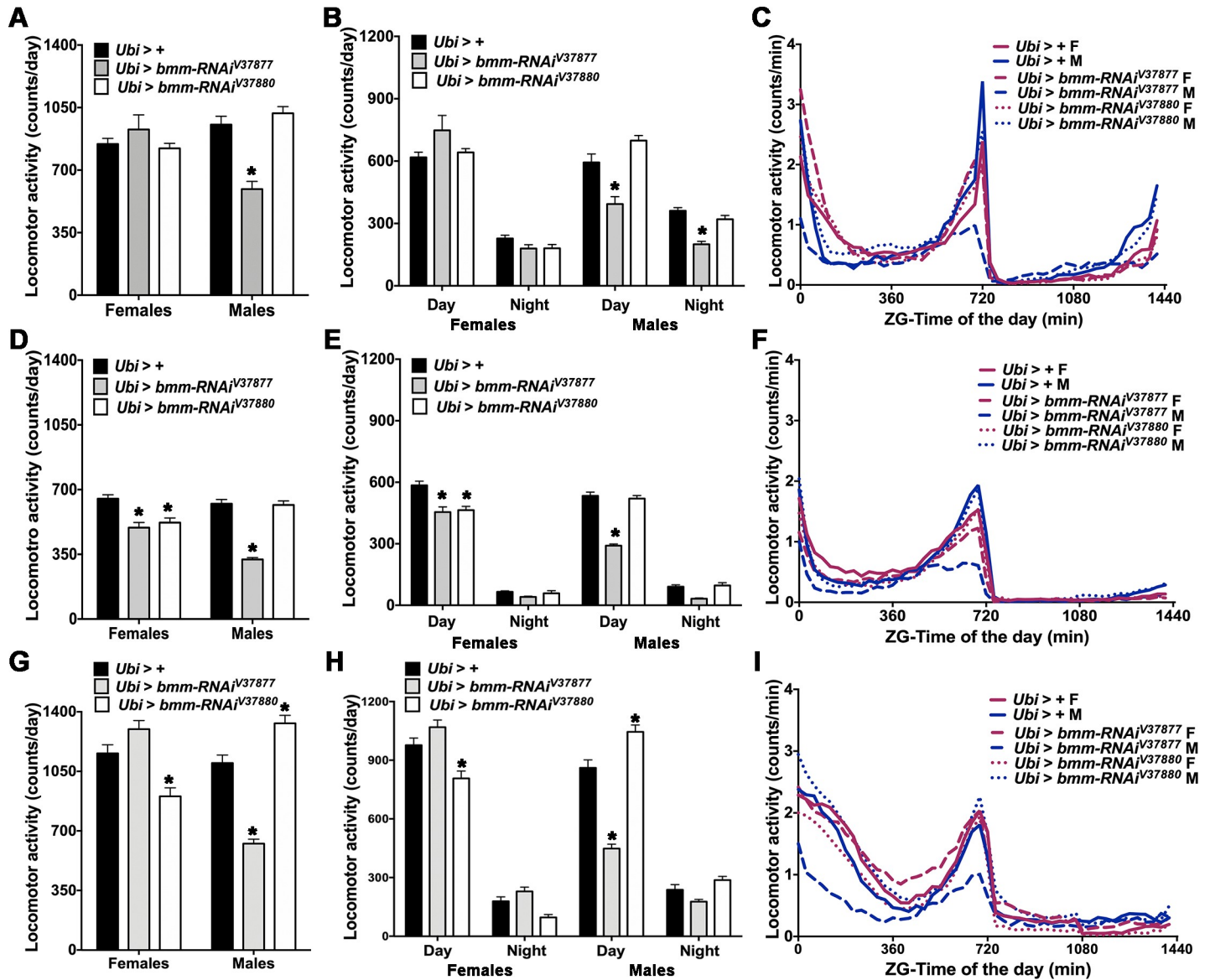


Fig 2. Locomotor activity in *Ubi > bmm-RNAi* flies. Offspring of *Ubi-Gal4* mated with GD control (*Ubi > +*) or *UAS-bmm-RNAi* flies (*Ubi > bmm-RNAi^{V37877}* and *Ubi > bmm-RNAi^{V37880}*) were used for the locomotor activity assay in normal feeding (a-c), normal feeding without wings (d-f) and starvation conditions (g-i). (a, d and g) Average of daily locomotor activity. (b, e and h) Average of locomotor activity during the daytime and nighttime. (c, f and i) Average activity profiles in Zeitgeber (ZG) time. Averages were calculated from 7 days of the behavior assays except for starvation, which was measured over 3 days. For this figure and Fig 3, “n” for normal feeding in females (F) and males (M) were: *Ubi > + F* (n = 49), *Ubi > + M* (n = 57), *Ubi > bmm-RNAi^{V37877} F* (n = 54), *Ubi > bmm-RNAi^{V37877} M* (n = 53), *Ubi > bmm-RNAi^{V37880} F* (n = 57) and *Ubi > bmm-RNAi^{V37880} M* (n = 62); “n” in normal feeding without wings were: *Ubi > + F* (n = 64), *Ubi > + M* (n = 62), *Ubi > bmm-RNAi^{V37877} F* (n = 56), *Ubi > bmm-RNAi^{V37877} M* (n = 55), *Ubi > bmm-RNAi^{V37880} F* (n = 58) and *Ubi > bmm-RNAi^{V37880} M* (n = 61); “n” in starvation were: *Ubi > + F* (n = 56), *Ubi > + M* (n = 42), *Ubi > bmm-RNAi^{V37877} F* (n = 54), *Ubi > bmm-RNAi^{V37877} M* (n = 52), *Ubi > bmm-RNAi^{V37880} F* (n = 63) and *Ubi > bmm-RNAi^{V37880} M* (n = 63). Asterisks indicate significant differences at *p* < 0.05 compared with the appropriate female or male control, following Tukey’s correction for multiple tests. Error bars are SEM. ANOVA tests are reported in S2 Table.

<https://doi.org/10.1371/journal.pone.0255198.g002>

RNAi^{V37877} females and starved *Ubi > bmm-RNAi^{V3880}* males slept less during the daytime and during the nighttime than the control (Fig 3I). Starved *Ubi > bmm-RNAi^{V37877}* males slept more during the daytime than the control (Fig 3I). In contrast, starved *Ubi > bmm-RNAi^{V37880}* males slept less during the daytime and nighttime than the corresponding control. Thus, effects of *bmm* expression on sleep patterns are condition-dependent and sex-dependent and vary with the extent of reduction in gene expression in the different RNAi lines.

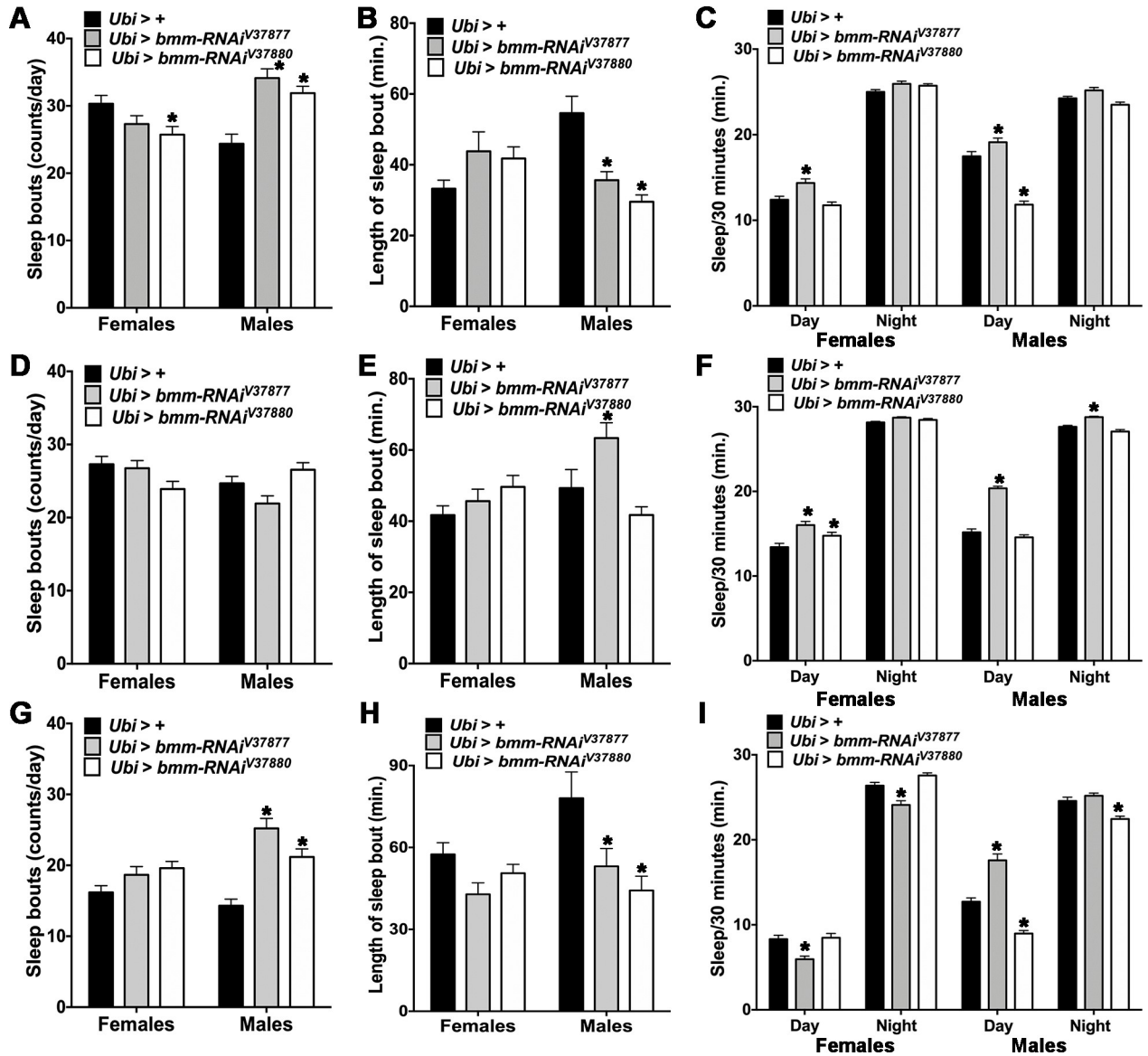


Fig 3. Sleep behavior in *Ubi > bmm-RNAi* flies. Offspring of *Ubi-Gal4* mated with GD control (*Ubi > +*) or *UAS-bmm-RNAi* flies (*Ubi > bmm-RNAi^{V37877}* and *Ubi > bmm-RNAi^{V37880}*) were used for the sleep assay in normal feeding (a-c), normal feeding without wings (d-f) and starvation conditions (g-i). (a, d and g) Average number of sleep bouts. (b, e and h) Average length of sleep bout. (c, f and i) Average sleep during the daytime and the nighttime. Sleep was calculated using the standard definition of a continuous period of inactivity lasting at least 5 minutes, and average was calculated from 7 days of behavior assay except for starvation, which was measured over 3 days, and recalculated to periods of 30 minutes of sleep. Asterisks indicate significant differences at $p < 0.05$ compared with the appropriate female or male control, following Tukey's correction for multiple tests. Error bars are SEM. ANOVA tests are reported in S3 Table.

<https://doi.org/10.1371/journal.pone.0255198.g003>

bmm downregulation in the fat body or oenocytes is sufficient to affect locomotor activity

Since the fat body and oenocytes are the two main tissues for triglyceride metabolism, we asked whether reduction of *bmm* expression specifically in these tissues could account for the observed effects on locomotor activity and sleep (S1 and S2 Figs, and S4 and S5 Tables). We combined *UAS-bmm-RNAi* with *Lsp2-Gal4* to down-regulate *bmm* in the fat body, and with *Dsat1-Gal4* and *Ok72-Gal4* to down-regulate *bmm* in oenocytes. Females of both *Lsp2 > bmm-RNAi* lines had

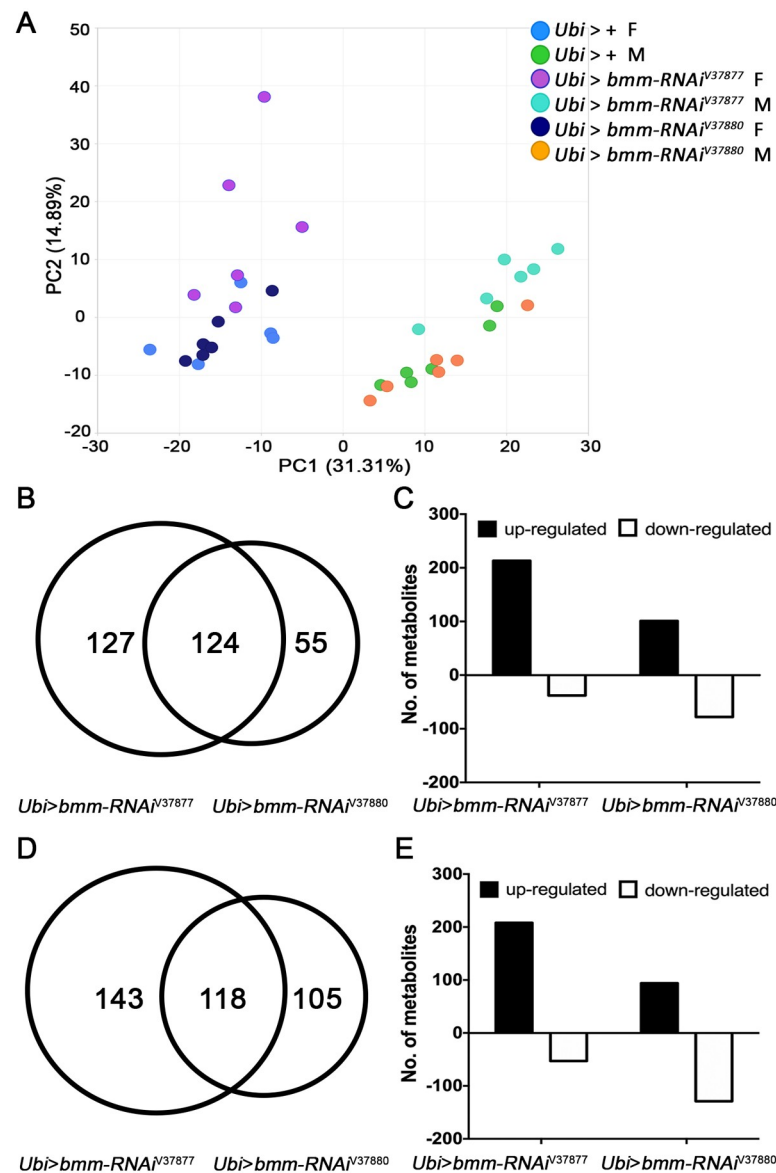


Fig 4. Metabolites with altered abundance levels in *Ubi* > *bmm-RNAi* flies. Offspring of *Ubi-Gal4* mated with GD control (*Ubi* > +) or *UAS-bmm-RNAi* flies (*Ubi* > *bmm-RNAi*^{V37877} and *Ubi* > *bmm-RNAi*^{V37880}) were used for metabolome analysis. F1 6-day-old adult females (F) and males (M) were used for the metabolomic profiles (n = 6). ANOVA contrasts were used to identify metabolites that differed significantly between experimental groups and corresponding controls at $p \leq 0.05$ (q-value is reported in S1 Dataset). (a) Principal component analysis of variation in the composition of the metabolome of flies in which *bmm* is downregulated and control flies. (b) Venn diagram of metabolites that significantly changed in *Ubi* > *bmm-RNAi* females compared with controls. (c) Number of metabolites that significantly increased (black bars) and decreased (white bars) in *Ubi* > *bmm-RNAi* females compared with controls. (d) Venn diagram of metabolites that significantly changed in *Ubi* > *bmm-RNAi* males compared with controls. (e) Number of metabolites that significantly increased (black bars) and decreased (white bars) in *Ubi* > *bmm-RNAi* males compared with controls.

<https://doi.org/10.1371/journal.pone.0255198.g004>

higher total 24h locomotor activity than controls (S1A Fig) and were more active during the daytime (S1B Fig). In contrast, *Lsp2* > *bmm-RNAi*^{V37880} males had lower 24h activity than controls (S1A Fig) and were less active during the daytime (S1B and S1C Fig). Interestingly, females of both *Dsat1* > *bmm-RNAi* lines showed less total 24h activity (S1D Fig) and less daytime activity

than control flies (S1E and S1F Fig). This reduction in activity also occurred with *OK72 > bmm-RNAi^{V37880}* females (S1G–S1I Fig). Furthermore, *Dsat1 > bmm-RNAi^{V37880}* males had lower 24h activity (S1D Fig) and lower daytime activity than control flies (S1E Fig). Similarly, *Dsat1 > bmm-RNAi^{V37877}* males exhibited reduced daytime activity (S1E Fig).

Tissue-specific reduction in *bmm* expression affects sleep behavior

Lsp2 > bmm-RNAi females of both strains had more sleep bouts (S2A Fig) than control flies but their bouts were shorter (S2B Fig) and these flies slept less during the daytime (S2C Fig). Interestingly, females and males of both *bmm-RNAi* lines combined with the two oenocyte drivers were not affected in the number or length of sleep bouts (S2D, S2E, S2G and S2H Fig); however, females slept more during the daytime (S2F and S2I Fig). Moreover, *bmm-RNAi^{V37880}* males combined with both oenocyte drivers slept more during the daytime similar to *Dsat1 > bmm-RNAi^{V37877}* males (S2F and S2I Fig). Also, males of both *OK72 > bmm-RNAi* flies rested less in the nighttime (S2I Fig). Our results show that metabolic effects resulting from reduction of *bmm* expression in the fat body or oenocytes are sufficient to affect energy-dependent organismal phenotypes.

bmm downregulation affects the metabolome in a sex-dependent manner

To gain insights in the mechanisms by which suppression of *bmm* expression results in physiological effects, we performed a comprehensive metabolomic analysis. The metabolome is a proximal link between gene expression and organismal phenotypes. To assess to what extent disruption of triglyceride metabolism through reduction of *bmm* expression affects the metabolome, we performed global metabolomics analysis on 6-day old *Ubi > bmm-RNAi* flies reared under standard culture conditions. We identified 767 metabolites, consisting of 723 known compounds and 44 compounds of unknown structural identity (S1 Dataset). Principal components analysis (PCA) highlights sexual dimorphism of the metabolome, with males and females separated along Component 1 (31.1% of the variance between samples) and genotypes partially separated along Component 2 (12.4% of the variance) (Fig 4A). Therefore, we performed all metabolomic analyses separately for females and males in single comparisons or comparing both *bmm-RNAi* lines with the corresponding control (S1 Dataset). The metabolomes of *Ubi > bmm-RNAi^{V37877}* females and males differ more from their controls (251 and 261 altered metabolite levels, respectively) than *Ubi > bmm-RNAi^{V37880}* females and males (179 and 223 altered metabolite levels, respectively). However, there were quantitative changes in metabolites common to both genotypes: 124 in females and 118 in males (Fig 4B and 4D). The proportion of metabolites upregulated/downregulated was higher in *Ubi > bmm-RNAi^{V37877}* (213↑/38↓ in females and 208↑/53↓ in males) than *Ubi > bmm-RNAi^{V37880}* (101↑/78↓ in females and 94↑/129↓ in males) (Fig 4C and 4E). These data reveal sex-dependent effects on the metabolome. The genotypes with higher effects on the metabolome correlate with lower levels of *bmm* transcripts (RT-qPCR), and greater effects on lifespan, locomotor activity and sleep parameters.

We performed Metabolite Set Enrichment Analysis (MSEA) for differentially abundant metabolites of single comparisons (S2 Dataset: a-b and d-e) or comparisons of both *bmm-RNAi* lines (S2 Dataset: c and f) with corresponding controls. Overrepresentation analysis exhibited changes in metabolic pathways of lipids (e.g. “Fatty acid metabolism”), carbohydrates (e.g. “Glycogen metabolism” and “Glycolysis, gluconeogenesis and pyruvate metabolism”), amino acids (e.g. “Tryptophan metabolism” and “Glycine, serine and threonine metabolism”) and nucleotides (e.g. “Purine metabolism” and “Pyrimidine metabolism”) for all comparisons.

***bmm* downregulation alters lipid metabolism**

We analyzed 298 metabolites from 49 lipid metabolism sub-pathways in flies in which *bmm* expression was suppressed compared to controls (S3 Fig). *Ubi > bmm-RNAi^{V37877}* females experienced more changes in metabolite levels (69, 57↑/12↓) than *Ubi > bmm-RNAi^{V37880}* females (60, 25↑/35↓). Conversely, *Ubi > bmm-RNAi^{V37877}* males had fewer changes in metabolite levels (76, 58↑/18↓) than *Ubi > bmm-RNAi^{V37880}* males (125, 44↑/81↓).

Our metabolomic analysis revealed significant decreases in almost all free fatty acids and monoacylglycerols evaluated in *Ubi > bmm-RNAi^{V37880}* males and in two lipid metabolites of *Ubi > bmm-RNAi^{V37880}* females (Fig 5). *Ubi > bmm-RNAi^{V37877}* males also showed decreases in the same lipid species, but the relative decreases failed to meet the threshold of significance (S1 Dataset). We also observed significant decreases in many acylcarnitine species in both sexes of *Ubi > bmm-RNAi^{V37880}* (Fig 6), indicating a deficiency in fatty acid transport into the mitochondria. These observations correlate with lipid enrichment analysis of differentially abundant metabolites which highlight “Fatty acyls” as the most prominent group (S3 Dataset) in all comparisons versus control.

We observed significant increases in several unsaturated diacylglycerol species (Fig 5), which suggests that conversion of triacylglycerol to diacylglycerol can occur in mutants with reduced expression of *bmm*, but that further breakdown of diacylglycerols is impaired. *Drosophila* utilizes a dual lipolytic strategy for fat mobilization, where Bmm seems to support the basal demands of lipolysis, while AkhR signaling, a cAMP-induced GPCR/PKA pathway, initiates the lipolytic response system that supports rapid fat mobilization [19,27]. Indeed, we observed significantly higher levels of cAMP in *bmm* knock-down females (S1 Dataset). Thus, the increase in long-chain diacylglycerols (DAGs), which are the most abundant DAGs in the fat body, brain and gut [28] in *Ubi > bmm-RNAi^{V37877}* females and males could indicate that *bmm* knockdown causes a switch to a second lipolytic system to compensate for the energy demands when *bmm* is expressed at low levels during normal feeding. Whereas changes in diacylglycerol species are correlated for males and females, overall changes in abundances of other lipid metabolites are sexually dimorphic with females counteracting the reduction in *bmm* more efficiently (Fig 5), as reported in other studies [25]. We also observed a significant increase in phosphatidylcholine (PC) and phosphatidylethanolamine (PE) levels (S1 Dataset), suggesting increased activity of phospholipase C or increased *de novo* synthesis of PC and PE.

Carbohydrate metabolism may compensate for lipid impairment in *bmm* knockdown flies

Impairment of lipid mobilization for energy production resulted in marked changes in the intermediates of the glycolysis pathway and the tricarboxylic acid (TCA) cycle in both *bmm* knockdown strains (Fig 7 and S2 Dataset). We evaluated 47 metabolites from 9 carbohydrate metabolism sub-pathways (S4 Fig). The same number of metabolites showed changes in abundance in *Ubi > bmm-RNAi^{V37877}* females (15, 12↑/3↓) and in *Ubi > bmm-RNAi^{V37880}* females (15, 10↑/5↓). However, more carbohydrate metabolites showed altered abundances in *Ubi > bmm-RNAi^{V37877}* males (22, 19↑/3↓) than in *Ubi > bmm-RNAi^{V37880}* males (11, 8↑/3↓). We observed more changes in metabolites associated with energy metabolism in *Ubi > bmm-RNAi^{V37877}* females than any other genotypes (S5 Fig). Our data indicate that altered carbohydrate metabolism in the *bmm* knockdown strains could compensate for impaired lipid mobilization.

Subpathway	Metabolite	<i>Ubi > bmm-RNAi / Ubi > +</i>			<i>Ubi > bmm-RNAi / Ubi > +</i>			
		V37877-F	V37880-F	V37877-F + V37880-F	V37877-M	V37880-M	V37877-M + V37880-M	
Medium Chain Fatty Acid	(2 or 3)-decenoate (10:1n7 or n8)	1.02	0.84	0.93	0.83	0.74	0.78	
	laurate (12:0)	1.33	0.66	1	0.82	0.5	0.66	
Long Chain Saturated Fatty Acid	myristate (14:0)	1.13	0.81	0.97	0.46	0.26	0.36	
	palmitate (16:0)	1.32	1.01	1.17	0.64	0.37	0.51	
	margarate (17:0)	1.72	1.19	1.46	0.46	0.23	0.34	
	stearate (18:0)	1.3	1.17	1.24	0.53	0.37	0.45	
	nonadecanoate (19:0)	2.86	1.2	2.03	0.2	0.12	0.16	
	arachidate (20:0)	3.67	1.74	2.71	0.25	0.17	0.21	
	palmitoleate (16:1n7)	1.06	0.92	0.99	0.41	0.27	0.34	
Long Chain Monounsaturated Fatty Acid	10-heptadecenoate (17:1n7)	1.37	1.22	1.3	0.21	0.13	0.17	
	oleate/vaccenate (18:1)	1.12	0.93	1.03	0.45	0.29	0.37	
	10-nonadecanoate (19:1n9)	1.83	0.86	1.34	0.28	0.12	0.2	
	eicosenoate (20:1)	2.12	1.3	1.71	0.36	0.15	0.26	
	erucate (22:1n9)	3.93	1.63	2.78	0.28	0.17	0.22	
	tetradecadienoate (14:2)*	2.81	0.61	1.71	1.47	0.92	1.2	
Long Chain Polyunsaturated Fatty Acid	hexadecatrienoate (16:3n3)	1.51	0.9	1.2	0.96	0.53	0.74	
	linoleate (18:2n6)	1.28	0.84	1.06	0.36	0.17	0.26	
	linolenate [alpha or gamma; (18:3n3 or 6)]	1.84	0.91	1.38	0.37	0.13	0.25	
	dihomo-linoleate (20:2n6)	1.83	1.65	1.74	0.38	0.19	0.29	
	1-myristoylglycerol (14:0)	0.97	0.76	0.86	0.28	0.21	0.25	
Monoacylglycerol	1-myristoleoylglycerol (14:1)	1.23	0.6	0.92	0.28	0.17	0.22	
	1-pentadecanoylglycerol (15:0)	1.65	1.36	1.51	0.22	0.13	0.17	
	1-palmitoylglycerol (16:0)	3.22	1.5	2.36	0.44	0.27	0.36	
	1-palmitoleoylglycerol (16:1)*	1.83	1.06	1.45	0.22	0.1	0.16	
	1-oleoylglycerol (18:1)	3.61	1.36	2.49	0.6	0.2	0.4	
	1-linoleoylglycerol (18:2)	6.06	1.43	3.74	0.5	0.09	0.3	
	1-linolenoylglycerol (18:3)	5.35	1.07	3.21	0.84	0.13	0.48	
	2-myristoylglycerol (14:0)	0.96	0.68	0.82	0.36	0.32	0.34	
	2-palmitoleoylglycerol (16:1)*	1.2	0.82	1.01	0.38	0.21	0.3	
	2-oleoylglycerol (18:1)	4.61	1.17	2.89	0.4	0.23	0.32	
	2-linoleoylglycerol (18:2)	5.65	1.48	3.56	0.42	0.1	0.26	
	Diacylglycerol	diacylglycerol (12:0/18:1, 14:0/16:1, 16:0/14:1) [2]*	0.69	0.7	0.69	0.78	0.97	0.87
		diacylglycerol (16:1/18:2 [2], 16:0/18:3 [1])*	1.74	0.92	1.33	1.94	1.2	1.57
		palmitoleoyl-linoleoyl-glycerol (16:1/18:2) [1]*	2.1	0.72	1.41	1.69	0.83	1.26
oleoyl-linoleoyl-glycerol (18:1/18:2) [2]		2.91	1.09	2	2.51	1.3	1.9	
linoleoyl-linolenoyl-glycerol (18:2/18:3) [2]*		1.74	1	1.37	1.23	1	1.11	

Fig 5. Compounds of lipid metabolism with altered levels of abundance in *Ubi > bmm-RNAi* flies. Heat map of changes in biochemicals of lipid metabolism in flies in which *bmm* is downregulated (*Ubi > bmm-RNAi*) compared with control flies (*Ubi > +*). For this graph and the graphs below, we performed a single comparison of each strain with its corresponding control for females (V37877-F and V37880-F) and males (V37877-M and V37880-M). Also, we performed a comparison of both strains with their corresponding controls for females (V37877-F + V37880-F) and males (V37877-M + V37880-M). Red and dark blue represent the metabolites that increased and decreased respectively at $p \leq 0.05$, light red and light blue represent the metabolites that increased and decreased respectively at $0.05 \leq p \leq 0.1$ (q-value is reported in S1 Dataset). Asterisks indicate compounds that have not been confirmed based on a standard.

<https://doi.org/10.1371/journal.pone.0255198.g005>

bmm downregulation results in changes in amino acid and nucleotide metabolic pathways

The shifts in energy metabolism described above are accompanied by changes in intermediaries of amino acid and peptide metabolism pathways (S6 and S7 Figs, and S2 Dataset). We

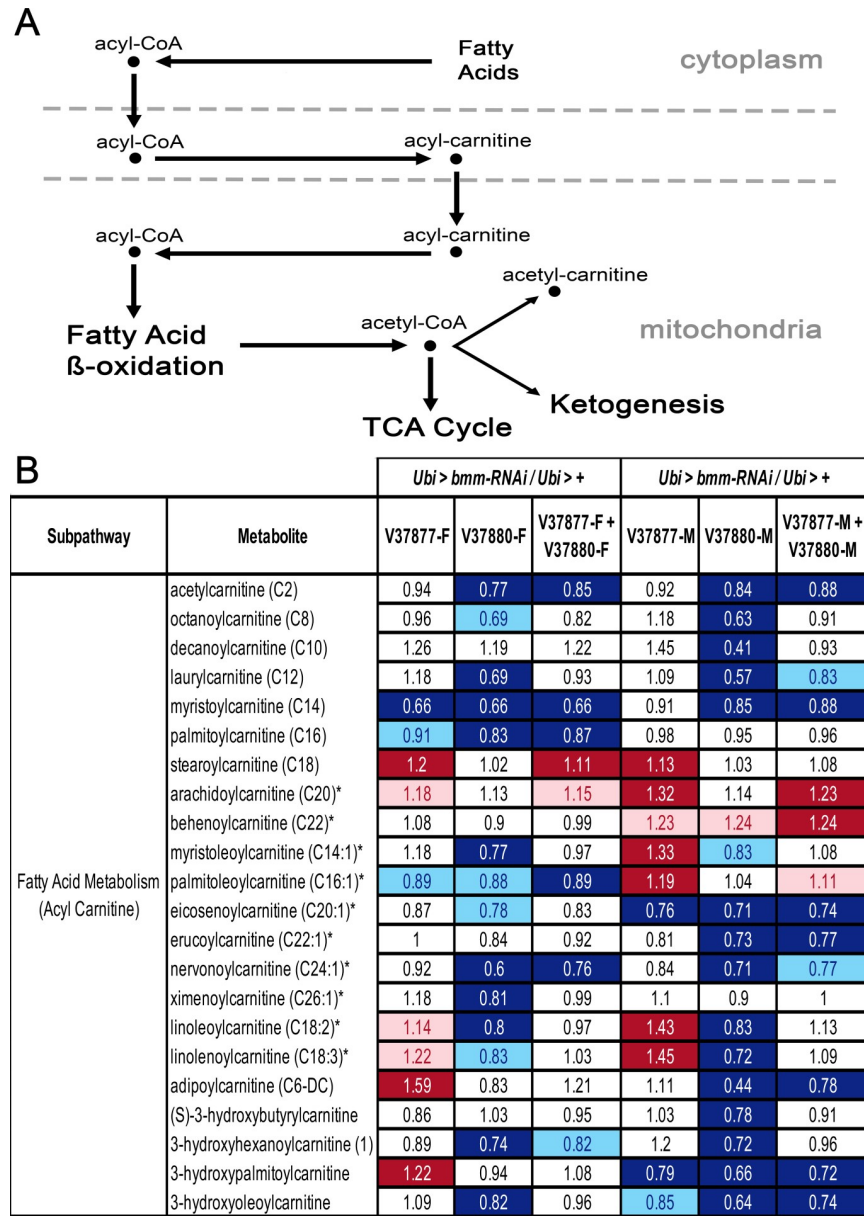


Fig 6. Compounds of acyl carnitine/fatty acid metabolism with altered abundance levels in *Ubi* > *bmm-RNAi* flies. (a) Diagram of the acyl carnitine/fatty acid metabolic pathway, highlighting the role of carnitine in facilitating transport of fatty acids into the mitochondria for fatty acid oxidation. (b) Heat map of changes in biochemicals of acyl carnitine/fatty acid metabolism in flies in which *bmm* is downregulated (*Ubi* > *bmm-RNAi*) compared with control flies (*Ubi* > +). Red and dark blue represent the metabolites that increased and decreased respectively at $p \leq 0.05$, light red and light blue represent the metabolites that increased and decreased respectively at $0.05 \leq p \leq 0.1$ (q-value is reported in S1 Dataset). Asterisks indicate compounds that have not been confirmed based on a standard.

<https://doi.org/10.1371/journal.pone.0255198.g006>

evaluated 175 compounds in 14 amino acid metabolic pathways. *Ubi* > *bmm-RNAi*^{V37877} females had altered quantities of 65 metabolites (58↑/7↓), while only 39 metabolites changed (27↑/12↓) in *Ubi* > *bmm-RNAi*^{V37880} females. *Ubi* > *bmm-RNAi*^{V37877} males showed changes in 64 metabolites (54↑/10↓), while *Ubi* > *bmm-RNAi*^{V37880} males only showed alterations in 32 compounds (18↑/14↓).

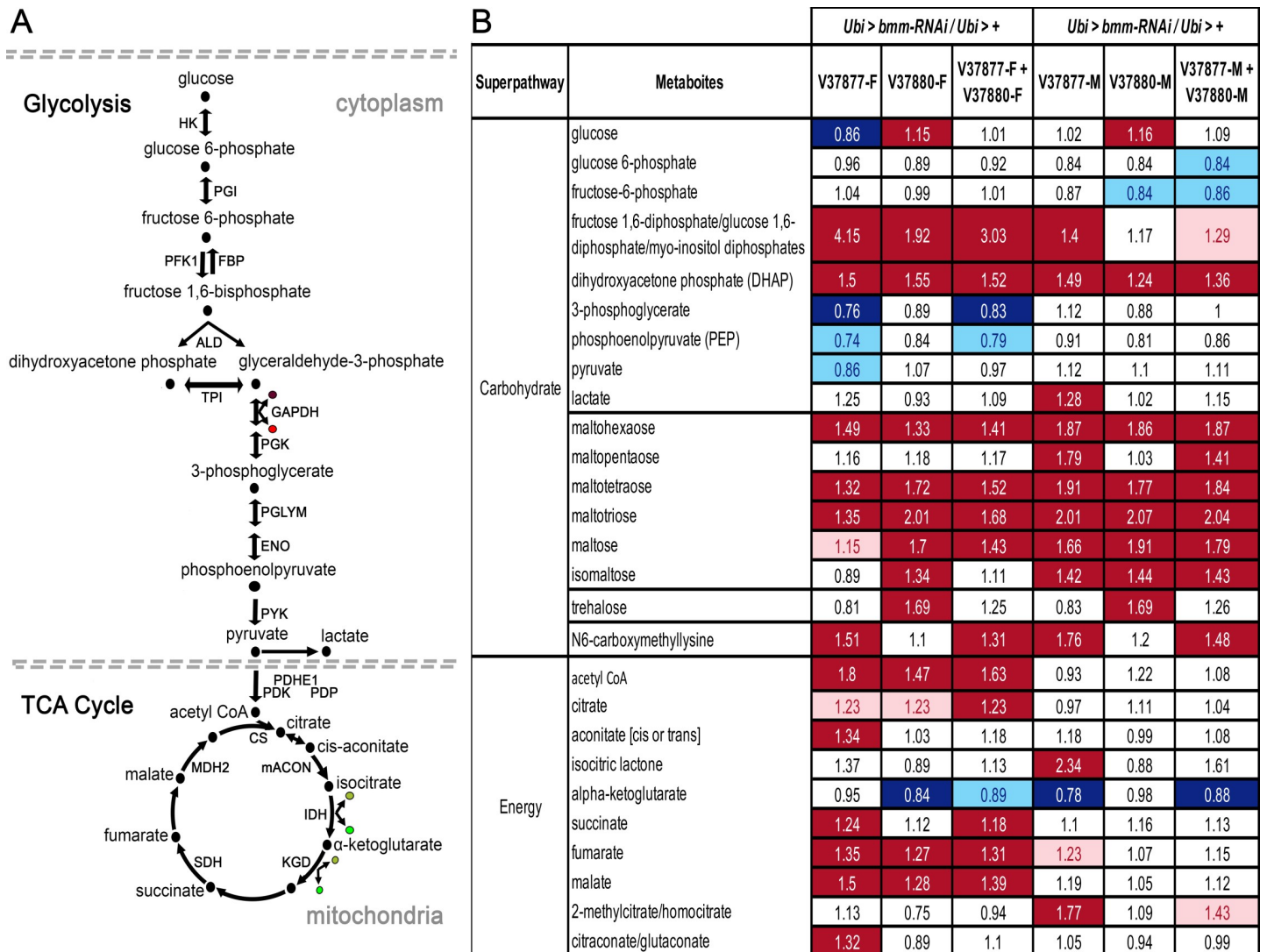


Fig 7. Metabolites of glycolysis and the TCA cycle with altered abundance levels in *Ubi > bmm-RNAi* flies. (a) Diagram of the glycolysis pathway and the TCA cycle. Black dots represent intermediates in the pathways and the enzymes in the reactions are marked with arrows and their initials: HK = Hexokinase, PGI = Phosphoglucose isomerase, FBP = Fructose 1,6-bisphosphatase, PFK = Phosphofructokinase, ALD = Aldolase, TPI = Triosephosphate isomerase, GAPDH = Glyceraldehyde-3-phosphate dehydrogenase, PGK = Phosphoglycerate kinase, PGLYM = Phosphoglyceromutase, ENO = Enolase, PYK = Pyruvate kinase, PDHE1 = Pyruvate dehydrogenase E1, PDK = Pyruvate dehydrogenase kinase, PDP = Pyruvate dehydrogenase phosphatase, CS = Citrate synthase, mACON = Mitochondrial aconitase, IDH = Isocitrate dehydrogenase, KGD = alpha-ketoglutarate dehydrogenase, SDH = Succinate dehydrogenase, MDH2 = Malate dehydrogenase. Brown dots designate ADP, bright-red dots, ATP, opaque-green dots, NAD⁺ and bright-green dots, NADH. (b) Heat map of variation in intermediates of carbohydrate metabolism and TCA cycle with altered abundance levels in *bmm* down-regulated (*Ubi > bmm-RNAi*) and control flies (*Ubi > +*). Red and dark blue represent the metabolites that increased and decreased respectively at $p \leq 0.05$, light red and light blue represent the metabolites that increased and decreased respectively at $0.05 \leq p \leq 0.1$ (q-value is reported in S1 Dataset). Asterisks indicate compounds that have not been confirmed based on a standard.

<https://doi.org/10.1371/journal.pone.0255198.g007>

We also identified 76 metabolites from 9 nucleotide metabolism sub-pathways (S8 Fig). *Ubi > bmm-RNAi*^{V37877} flies showed more changes in levels of nucleotide intermediaries than *Ubi > bmm-RNAi*^{V37880} flies. In *Ubi > bmm-RNAi*^{V37877} females 65 metabolites underwent changes in abundance (58↑/7↓), whereas only 39 metabolites changed (27↑/12↓) in *Ubi > bmm-RNAi*^{V37880} females. In *Ubi > bmm-RNAi*^{V37877} males 64 metabolites showed altered levels of abundance (54↑/10↓) and levels of 32 metabolites changed in *Ubi > bmm-RNAi*^{V37880}

males (18↑/14↓). Thus, dysregulation of lipid metabolism has widespread consequences in the metabolome.

***bmm* knockdown alters neurotransmitter levels**

Motivated by the effects of *bmm* suppression on locomotion, sleep and lifespan, we explored changes in neurotransmitter levels resulting from *bmm* knockdown. We observed significant alterations, dependent on RNAi genotype and sex, of different neurotransmitters in *bmm* knockdown flies (S1 Dataset). Inhibition of the tryptophan-kynurenine (TRY-KYN) pathway increases N-acetylserotonin (NAS) levels, which has been associated with extended lifespan in *Drosophila* [29,30]. Indeed, we found reduced levels of NAS in both sexes of *bmm* knockdown flies and elevated TRY-KYN pathway metabolites in line with their reduced lifespan (Fig 1C). In addition, levels of serotonin were increased in *bmm* knockdown males. Furthermore, dopamine and its precursor L-DOPA are elevated in *bmm* knockdown flies. We also found altered levels of tyramine in *bmm* knockdown females and of acetylcholine in both sexes.

Discussion

We used RNAi-mediated suppression of *bmm*, which encodes triacylglyceride lipase in *Drosophila*, to explore the behavioral, physiological and metabolic consequences of disruption of lipid mobilization. We mitigated potential off-target effects using two different RNAi lines targeting *bmm* with no predicted off-target effects. Both RNAi constructs affected the same phenotypes, but with quantitative differences that largely correlated with their different efficacies in *bmm* suppression. The phenotypic differences between the two RNAi lines could be attributable to different amounts of knock down of *bmm* gene expression caused by differences in chromatin accessibility between the two insertion sites, because the *P*-element RNAi constructs directly affect the insertion site, or both. However, phenotypic similarities between the RNAi lines are most parsimoniously attributable to direct effects of RNAi knock down of *bmm* expression. We observed pervasive sex differences in all organismal level phenotypes and in the metabolome, which is not surprising as sexual dimorphism has been reported for virtually all complex traits examined in *Drosophila* [15,31–33]. Reduction in expression of *bmm* affected locomotor activity and sleep patterns and resulted in widespread shifts in abundances of metabolites in a range of metabolic pathways. We note, however, that the metabolomic data were obtained at a single time point during the circadian cycle and at a single age. Sampling at different times during the day and night and at different ages may provide more comprehensive information on the circadian dynamics of the effects of *bmm* suppression on the metabolome.

A previous study showed that a restricted larval diet results in downregulation of *bmm* [34]. Adults that emerged from these larvae had increased levels of triglycerides and were more resistant to starvation stress. This effect could be mimicked by targeted reduction of *bmm* levels in the larval fat body [34]. Reduction of *bmm* expression in the fat body in adult flies also protects against cardiac dysfunction during starvation and flies with reduced *bmm* expression during starvation have higher levels of metabolites involved in energy metabolism, and high levels of diacylglycerol [35], which is also upregulated under our experimental conditions (Fig 5).

Tissue-specific inhibition of *bmm* in the fat body and oenocytes is sufficient to affect locomotor activity and sleep patterns

Our locomotor activity data show the strongest effect on locomotor activity both under normal feeding conditions and during food deprivation in *Ubi > bmm-RNAi^{V37877}* males, consistent

with the lowest level of *bmm* transcripts in these flies (Figs 1 and 2). Furthermore, *bmm* downregulation in fat body or oenocytes was sufficient to affect locomotor activity and sleep (S1 and S2 Figs). In females, however, effects on locomotor activity are in opposite directions when *bmm* is downregulated in the fat body and oenocytes. *bmm* function in the fat body is necessary for lipid utilization by oenocytes, and oenocytes are essential for lipid regulation, but the midgut can also provide TAGs to oenocytes [18]; thus, females might use another source of lipids when *bmm* is downregulated in fat body to compensate. These data suggest that *bmm* function in oenocytes is a limiting factor to obtain energy for locomotor activity in both sexes, but *bmm* function in the fat body is more important in males, such as it is in the somatic cells of the gonads [25].

The effect of *bmm* suppression in the fat body and oenocytes on locomotion and sleep was weaker than the effect observed with a ubiquitous *Gal4* driver. This could be due to less effective suppression of *bmm* with these tissue-specific drivers or to intact lipolysis in other tissues that may contribute energy towards locomotion and normal sleep patterns. *bmm* is expressed in different tissues [23]; indeed, neuronal function of *bmm* is necessary to regulate sex-dependent triglyceride breakdown [25]. Sleep disruption is associated with increased weight and lipids in humans [36,37] but it is not clear if dysregulation of lipids affects sleep [38].

Carbohydrate metabolism may compensate for lipid impairment in *bmm* knockdown flies

We observed significant increases in carbohydrates, such as maltohexaose and maltopentaose, as well as glucose and trehalose levels in *Ubi > bmm-RNAi^{V37880}* flies. Trehalose is a disaccharide consisting of two glucose molecules, which serves as a source for glucose in the hemolymph [39]. Since *Ubi > bmm-RNAi^{V37880}* flies exhibited a severely impaired lipid mobilization phenotype, the fat body in these flies may generate trehalose to support energy demands and buffer the levels of glucose. Alternatively, decreased uptake and utilization of trehalose from the circulation could account for its accumulation in flies in which *bmm* expression is suppressed.

Ubi > bmm-RNAi^{V37877} flies showed a significant increase in the advanced-glycation end product (AGE) N6-carboxymethyllysine, which serves as a biomarker of high blood glucose levels in humans; this might suggest a diabetes-like phenotype. High levels of AGEs together with high-fat diet produces liver dysfunction in mice [40], and liver dysfunction produces AGEs accumulation in humans [41]. Whether AGEs represent dysfunction of the fat body in *Ubi > bmm-RNAi^{V37877}* flies is not clear, since glucose did not increase significantly in these flies, nor did they exhibit an increase in trehalose production by the fat body. These results provide a framework for future studies on compensatory metabolic mechanisms through manipulation of carbohydrate metabolism in the *bmm* mutant.

bmm knockdown alters neurotransmitter levels

Inhibition of *bmm* expression results in elevated levels of the neurotransmitters serotonin and dopamine, which may account for impairment of locomotor activity and altered sleep patterns [42–44]. Serotonin 5-HT_{1A} receptors in *Drosophila* are required for insulin-producing cells to regulate lipid content [45]. Interestingly, the quantity of serotonin transporters (SERT) in the midbrain correlates with body-mass index in humans, with a negative correlation in people with obesity and a positive correlation in non-obesity individuals. This correlation supports the idea that serotonin may play a role in the reward

system of food intake [46]. Also, increased levels of dopamine can lead to a reduction in striatal D2-dopamine receptors in humans with obesity through habituation [47]. Causal relationships between neurotransmitter levels and *bmm*-sensitive phenotypes in flies requires assessment in future experiments.

Conclusions

Impairment of fatty acid mobilization results in a shift in intermediary metabolism toward utilization of carbohydrates as an energy source. In addition, amino acid, nucleotide, and neurotransmitter metabolic pathways are affected by disruption of lipid catabolism. This altered metabolic state gives rise to changes in morphological and physiological organismal phenotypes. Because pathways of intermediary metabolism are conserved across phyla, studies on the *Drosophila* model are relevant to advancing our understanding of human metabolic disorders.

Materials and methods

Fly stocks

We obtained two w^{1118} ; *UAS-bmm-RNAi* lines (#37877 and #37880) and their GD control from the Vienna *Drosophila* Resource Center [48]. All *Gal4* driver lines were obtained from the Bloomington *Drosophila* Stock Center: w^* ; *Ubi-Gal4/CyO* (#32551) for ubiquitous expression, w^{1118} ; *Lsp2-Gal4* (#6357) for specific expression in fat body, and w^* ; *Dsat1-Gal4* (#65405) and w^* ; *OK72-Gal4* (#6486) for expression in oenocytes. Flies were reared on molasses-cornmeal medium (Nutri-Fly®) with propionic acid and Tegosept (Genesee Scientific, Inc.) added as fungicides. They were maintained at 25°C and a 12h:12h light-dark schedule (lights on at 6:00 am). Matings were performed with 6 pairs per vial and flies were maintained at a controlled population density. *UAS-bmm-RNAi* flies and control GD flies were crossed with *Ubi-Gal4/CyO*. The progeny with one copy of *Ubi-Gal4* and *UAS-bmm-RNAi* (*Ubi* > *bmm-RNAi*^{V37877} and *Ubi* > *bmm-RNAi*^{V37880}) or *Ubi-Gal4* and GD control background (*Ubi* > +), were subjected to RT-qPCR, lifespan assay, locomotor activity/sleep assay and metabolomic analysis.

RT-qPCR

Three biological replicates of 3 to 5-day old virgin females and males, with one copy of *Ubi-Gal4* and *UAS-bmm-RNAi* (*Ubi* > *bmm-RNAi*^{V37877} and *Ubi* > *bmm-RNAi*^{V37880}) or the GD control (*Ubi* > +), were anesthetized with CO₂ and frozen on dry ice. All flies were collected at the same time of day to avoid effects of circadian rhythms and stored at -80°C. Total RNA was extracted using the RNeasy Plus Mini Kit (Qiagen, Inc.) and single strand cDNA was generated with High-Capacity cDNA Reverse Transcription (Thermo Fisher, AB). We designed primers to generate a PCR fragment of 116 bp for *bmm* and 102 bp for *Gapdh1* (S4 Dataset). Relative quantification (RQ) was done using the 2^{-ΔΔCt} method with *Gapdh1* as internal control because it was stable across genotypes when comparing raw cycle thresholds (Tukey's test $p < 0.05$, $n = 9$). Three technical replicates were used for each sample, and qPCR was performed in a QuantStudio 3 instrument (Applied Biosystems).

Lifespan assay

We used mated flies with one copy of *Ubi-Gal4* and *UAS-bmm-RNAi* (*Ubi* > *bmm-RNAi*^{V37877} and *Ubi* > *bmm-RNAi*^{V37880}) or the GD control (*Ubi* > +) for lifespan assays. We set up 50 vials of molasses-cornmeal media with 3 males or 3 females for each genotype, transferred

them to fresh food every 2–3 days, and scored for survival daily. Flies that escaped during transfers or were stuck in the food were discarded from the analysis (S5 Dataset). Average life-span for each group was calculated and data are presented as mean \pm standard error.

Locomotor activity/sleep assay

w¹¹¹⁸; *UAS-bmm-RNAi* flies and control GD flies were crossed with the ubiquitous driver (*w^{*}*; *Ubi-Gal4/CyO*), the fat body driver (*w¹¹¹⁸*; *Lsp2-Gal4*) or oenocyte drivers (*w^{*}*; *OK72-Gal4* and *w^{*}*; *Dsat1-Gal4*). Offspring with one copy of driver-*Gal4* and *UAS-bmm-RNAi* or the GD control were subjected to activity monitoring using *Drosophila* Activity Monitors (DAMSystem3, TriKinetics Inc.), which record movement by counting interruptions of an infrared beam. Tubes were plugged with 2% agar and 5% sucrose for normal feeding assays and 1% agar for starvation assays [31].

Two-day old males and females of the three genotypes were collected simultaneously and unmated flies were used for the assay. Two full 32-tube replicates were analyzed for activity behavior for each sex and genotype (S6–S10 Datasets). The incubator followed a 12h day-12h night cycle and the activity behavior was recorded for 7 days in one-minute bins. Whole day activity, daytime/nighttime activity, average activity profiles, sleep bouts, sleep bout length and actograms were calculated using ShinyR-DAM [49] and data are presented as mean \pm standard error. Means were calculated from 7 days of recording except for starvation where only 3 days were recorded. Sleep was calculated using the standard definition of a continuous period of inactivity lasting at least 5 min [50]. Sleep events were identified using a sliding window algorithm of 5 min width and 1 min sliding interval, then averaged over all individual flies per condition.

Metabolomic analysis

Six replicates of ~150 6-day old females and males for each genotype (36 samples) were collected at the same time of day on dry ice and stored at -80°C. Unmated flies were used for metabolomic profiling by Metabolon, Inc., NC. Samples were prepared using the automated MicroLab STAR system from Hamilton Company, adding several recovery standards for quality control prior to the extraction process. Proteins were precipitated with methanol under vigorous shaking (Glen Mills GenoGrinder 2000) for 2 min., followed by centrifugation (to remove protein, dissociate small molecules bound to protein or trapped in the precipitated protein matrix, and to recover chemically diverse metabolites). The extract was divided into five fractions: two for analysis by two separate RP/UPLC-MS/MS methods with positive ion mode ESI, one for analysis by RP/UPLC-MS/MS with negative ion mode ESI, one for analysis by HILIC/UPLC-MS/MS with negative ion mode ESI, and one sample was reserved for backup. Organic solvent was removed placing samples on a TurboVap (Zymark) and the sample extracts were stored overnight under nitrogen before preparation for analysis. Metabolites were extracted from the flies and loaded in an equivalent manner across the analytical platforms and the values for each metabolite were normalized based on Bradford protein concentrations.

Metabolon's hardware and software were used for raw data extraction, peak-identification, and quality control processing. Compounds were identified by comparison to library entries of purified standards (or recorded as unknown entities) and peaks were quantified using area under the curve. Data normalization was performed to correct variation from instrument inter-day tuning differences. Each compound was corrected in run day blocks by registering the medians to equal one (1.00) and normalizing each data point proportionately. The detailed procedure for metabolomic profiling from Metabolon Inc. has been described previously [15].

Metabolic networks and metabolite set enrichment analysis

Metabolic networks are rendered using a private custom software application made by Metabolon that is based on the Cytoscape application. This software uses the Cytoscape JS toolkit and the D3 JavaScript library [51,52] and is available in MyMetabolon portal. Metabolite set enrichment analysis of global metabolic pathways (S2 Dataset) was performed with Fisher's exact tests, mapping the list of differentially abundant metabolites to the Metabolon library, and the FDR method was used for correction of multiple comparisons. Enrichment analysis for lipid chemical structure (S3 Dataset) was done using the PubChem-IDs lists as input in the "Enrichment Analysis" web tool of MetaboAnalyst 5.0 (<https://www.metaboanalyst.ca>). Mapped metabolites in the Human Metabolome Database (HMDB) were used for over-representation analysis of lipid structure comparing to the super-class dataset.

Statistical analyses

Two-way ANOVA tests were performed for RT-qPCR and locomotor activity/sleep, followed by Tukey's multiple testing correction ($p < 0.05$) to assess statistically significant results (S1–S5 Tables). For lifespan, we performed a two-way mixed model ANOVA with genotype and sex as fixed effects and vial as random effect, followed by Dunnett's correction for multiple tests ($p < 0.05$) (S1 Table). Metabolites profiled by mass spectroscopy in *Ubi > bmm-RNAi* females and males were analyzed separately with one-way ANOVA. ANOVA contrasts between experimental groups and controls were performed using two approaches: single comparisons of each strain with the corresponding control (V37877-F, V37880-F, V37877-M and V37880-M) or comparisons of both strains with the proper control (V37877-F + V37880-F and V37877-M + V37880-M). Mean, p-values and q-values, and the magnitude of changes are in S1 Dataset. Statistics and graphs were built on Prism 6 (GraphPad Software), R (R 3.6.1) and JMP (SAS Institute Inc.).

Supporting information

S1 Fig. Locomotor activity in *bmm-RNAi* lines expressed in fat-body and oenocytes. GD control and *UAS-bmm-RNAi* flies were mated with *Lsp2-Gal4* (a-c), *Dsat1-Gal4* (d-f) and *OK72-Gal4* (g-i), and F1-flies were used for the assay in normal feeding. (a, d and g) Average of whole-day locomotor activity. (b, e and h) Average of locomotor activity during the daytime and nighttime. (c, f and i) Average activity profiles in Zeitgeber time. Averages were calculated from 7 days of behavior assay. For this and S2 Fig, "n" for females (F) and males (M) were: *Lsp2 > + F* (n = 60), *Lsp2 > + M* (n = 63), *Lsp2 > bmm-RNAi^{V37877} F* (n = 55), *Lsp2 > bmm-RNAi^{V37877} M* (n = 57), *Lsp2 > bmm-RNAi^{V37880} F* (n = 57), *Lsp2 > bmm-RNAi^{V37880} M* (n = 61), *Dsat1 > + F* (n = 62), *Dsat1 > + M* (n = 63), *Dsat1 > bmm-RNAi^{V37877} F* (n = 63), *Dsat1 > bmm-RNAi^{V37877} M* (n = 63), *Dsat1 > bmm-RNAi^{V37880} F* (n = 63), *Dsat1 > bmm-RNAi^{V37880} M* (n = 63), *OK72 > + F* (n = 58), *OK72 > + M* (n = 54), *OK72 > bmm-RNAi^{V37877} F* (n = 61), *OK72 > bmm-RNAi^{V37877} M* (n = 60), *OK72 > bmm-RNAi^{V37880} F* (n = 63) and *OK72 > bmm-RNAi^{V37880} M* (n = 61). Asterisks indicate significant differences at $p < 0.05$ compared with the appropriate female or male control, following Tukey's correction for multiple tests. Error bars are SEM. ANOVA tests are reported in S4 Table. (JPG)

S2 Fig. Sleep behavior in *bmm-RNAi* lines expressed in fat-body and oenocytes. GD control and *UAS-bmm-RNAi* flies were mated with *Lsp2-Gal4* (a-c), *Dsat1-Gal4* (d-f) and *OK72-Gal4* (g-i), and F1-flies were used for the assay in normal feeding. (a, d and g) Average number of sleep bouts. (b, e and h) Average length of sleep bout. (c, f and i) Average sleep during the

daytime and the nighttime. Sleep was calculated using the standard definition of continuous period of inactivity lasting at least 5 minutes. Averages were calculated from 7 days of behavior assay and recalculated to periods of 30 minutes of sleep. Asterisks indicate significant differences at $p < 0.05$ compared with the appropriate female or male control, following Tukey's correction for multiple tests. Error bars are SEM. ANOVA tests are reported in [S5 Table](#). (JPG)

S3 Fig. Lipid metabolism network with biochemicals with significantly altered abundances in *Ubi* > *bmm*-RNAi flies. (a) Metabolites that significantly changed in *Ubi* > *bmm*-RNAi^{V37877} females compared with control females. (b) Metabolites that significantly changed in *Ubi* > *bmm*-RNAi^{V37880} females compared with control females. (c) Metabolites that significantly changed in *Ubi* > *bmm*-RNAi^{V37877} males compared with control males. (d) Metabolites that significantly changed in *Ubi* > *bmm*-RNAi^{V37880} males compared with control males. Yellow nodes represent the sub-pathways analyzed (see [S1 Dataset](#)). Red and dark blue represent the metabolites that increased and decreased respectively at $p \leq 0.05$, light red and light blue represent the metabolites that increased and decreased respectively at $0.05 \leq p \leq 0.1$, and size of circles represent the magnitude of change. ANOVA contrasts were used to identify metabolites that differed significantly between experimental groups and proper controls, and q-value is reported in [S1 Dataset](#). (JPG)

S4 Fig. Carbohydrate metabolism network with biochemicals with significantly altered abundances in *Ubi* > *bmm*-RNAi flies. (a) Metabolites that significantly changed in *Ubi* > *bmm*-RNAi^{V37877} females compared with control females. (b) Metabolites that significantly changed in *Ubi* > *bmm*-RNAi^{V37880} females compared with control females. (c) Metabolites that significantly changed in *Ubi* > *bmm*-RNAi^{V37877} males compared with control males. (d) Metabolites that significantly changed in *Ubi* > *bmm*-RNAi^{V37880} males compared with control males. Yellow nodes represent the sub-pathways analyzed (see [S1 Dataset](#)). Red and dark blue represent the metabolites that increased and decreased respectively at $p \leq 0.05$, light red and light blue represent the metabolites that increased and decreased respectively at $0.05 \leq p \leq 0.1$, and size of circles represent the magnitude of change. ANOVA contrasts were used to identify metabolites that differed significantly between experimental groups and proper controls, and q-value is reported in [S1 Dataset](#). (JPG)

S5 Fig. Network of energy metabolites with significantly altered abundances in *Ubi* > *bmm*-RNAi flies. (a) Metabolites that significantly changed in *Ubi* > *bmm*-RNAi^{V37877} females compared with control females. (b) Metabolites that significantly changed in *Ubi* > *bmm*-RNAi^{V37880} females compared with control females. (c) Metabolites that significantly changed in *Ubi* > *bmm*-RNAi^{V37877} males compared with control males. (d) Metabolites that significantly changed in *Ubi* > *bmm*-RNAi^{V37880} males compared with control males. Yellow nodes represent the sub-pathways analyzed (see [S1 Dataset](#)). Red and dark blue represent the metabolites that increased and decreased respectively at $p \leq 0.05$, light red and light blue represent the metabolites that increased and decreased respectively at $0.05 \leq p \leq 0.1$, and size of circles represent the magnitude of change. ANOVA contrasts were used to identify metabolites that differed significantly between experimental groups and proper controls, and q-value is reported in [S1 Dataset](#). (JPG)

S6 Fig. Amino acid metabolism network with intermediates with significantly altered abundances in *Ubi* > *bmm*-RNAi flies. (a) Metabolites that significantly changed in *Ubi* >

bmm-RNAi^{V37877} females compared with control females. (b) Metabolites that significantly changed in *Ubi* > *bmm*-RNAi^{V37880} females compared with control females. (c) Metabolites that significantly changed in *Ubi* > *bmm*-RNAi^{V37877} males compared with control males. (d) Metabolites that significantly changed in *Ubi* > *bmm*-RNAi^{V37880} males compared with control males. Yellow nodes represent the sub-pathways analyzed (see [S1 Dataset](#)). Red and dark blue represent the metabolites that increased and decreased respectively at $p \leq 0.05$, light red and light blue represent the metabolites that increased and decreased respectively at $0.05 \leq p \leq 0.1$, and size of circles represent the magnitude of change. ANOVA contrasts were used to identify metabolites that differed significantly between experimental groups and proper controls, and q-value is reported in [S1 Dataset](#).

(JPG)

S7 Fig. Peptide metabolism network intermediates with significantly altered abundances in *Ubi* > *bmm*-RNAi flies.

(a) Metabolites that significantly changed in *Ubi* > *bmm*-RNAi^{V37877} females compared with control females. (b) Metabolites that significantly changed in *Ubi* > *bmm*-RNAi^{V37880} females compared with control females. (c) Metabolites that significantly changed in *Ubi* > *bmm*-RNAi^{V37877} males compared with control males. (d) Metabolites that significantly changed in *Ubi* > *bmm*-RNAi^{V37880} males compared with control males. Yellow nodes represent the sub-pathways analyzed (see [S1 Dataset](#)). Red and dark blue represent the metabolites that increased and decreased respectively at $p \leq 0.05$, light red and light blue represent the metabolites that increased and decreased respectively at $0.05 \leq p \leq 0.1$, and size of circles represent the magnitude of change. ANOVA contrasts were used to identify metabolites that differed significantly between experimental groups and proper controls, and q-value is reported in [S1 Dataset](#).

(JPG)

S8 Fig. Nucleotide metabolism network intermediates with significantly altered abundances *Ubi* > *bmm*-RNAi flies.

(a) Metabolites that significantly changed in *Ubi* > *bmm*-RNAi^{V37877} females compared with control females. (b) Metabolites that significantly changed in *Ubi* > *bmm*-RNAi^{V37880} females compared with control females. (c) Metabolites that significantly changed in *Ubi* > *bmm*-RNAi^{V37877} males compared with control males. (d) Metabolites that significantly changed in *Ubi* > *bmm*-RNAi^{V37880} males compared with control males. Yellow nodes represent the sub-pathways analyzed (see [S1 Dataset](#)). Red and dark blue represent the metabolites that increased and decreased respectively at $p \leq 0.05$, light red and light blue represent the metabolites that increased and decreased respectively at $0.05 \leq p \leq 0.1$, and size of circles represent the magnitude of change. ANOVA contrasts were used to identify metabolites that differed significantly between experimental groups and proper controls, and q-value is reported in [S1 Dataset](#).

(JPG)

S1 Table. ANOVA of RT-qPCR and lifespan of *Ubi* > *bmm*-RNAi flies.

(PDF)

S2 Table. ANOVAs of locomotor activity of *Ubi* > *bmm*-RNAi flies.

(PDF)

S3 Table. ANOVAs of sleep of *Ubi* > *bmm*-RNAi flies.

(PDF)

S4 Table. ANOVAs of locomotor activity of *bmm*-RNAi lines expressed in fat-body (*Lsp2-Gal4*) and oenocytes (*Dsat1-Gal4* and *OK72-Gal4*) in normal feeding.

(PDF)

S5 Table. ANOVAs of sleep of *bmm*-RNAi lines expressed in fat-body (*Lsp2-Gal4*) and oenocytes (*Dsat1-Gal4* and *OK72-Gal4*) in normal feeding.

(PDF)

S1 Dataset. Metabolome of *Ubi* > *bmm*-RNAi lines.

(XLSX)

S2 Dataset. Over-representation analysis of global metabolic pathways for differentially abundant metabolites on *Ubi* > *bmm*-RNAi lines.

(XLSX)

S3 Dataset. Overrepresentation analysis of lipids for differentially abundant metabolites on *Ubi* > *bmm*-RNAi lines.

(XLSX)

S4 Dataset. RT-qPCRs and internal control.

(XLSX)

S5 Dataset. Raw lifespan data of *Ubi* > *bmm*-RNAi flies.

(XLSX)

S6 Dataset. Average locomotor activity profiles.

(XLSX)

S7 Dataset. Average of 24h locomotor activity.

(XLSX)

S8 Dataset. Average of locomotor activity during the daytime and nighttime.

(XLSX)

S9 Dataset. Individual sleep during the daytime and nighttime.

(XLSX)

S10 Dataset. Individual activity/sleep bout raw data.

(XLSX)

Acknowledgments

We would like to thank Dr. Therese A. Markow for comments on the manuscript.

Author Contributions

Conceptualization: Nestor O. Nazario-Yepiz, Robert R. H. Anholt, Trudy F. C. Mackay.

Data curation: Nestor O. Nazario-Yepiz.

Formal analysis: Nestor O. Nazario-Yepiz, Vijay Shankar.

Funding acquisition: Robert R. H. Anholt, Trudy F. C. Mackay.

Investigation: Nestor O. Nazario-Yepiz, Jaime Fernández Sobaberas, Roberta Lyman, Marion R. Campbell, III.

Project administration: Robert R. H. Anholt, Trudy F. C. Mackay.

Supervision: Robert R. H. Anholt, Trudy F. C. Mackay.

Writing – original draft: Nestor O. Nazario-Yepiz.

Writing – review & editing: Nestor O. Nazario-Yepiz, Robert R. H. Anholt, Trudy F. C. Mackay.

References

1. Afshin A, Forouzanfar MH, Reitsma MB, Sur P, Estep K, Lee A, et al. Health effects of overweight and obesity in 195 countries over 25 years. *N. Engl. J. Med.* 2017; 377:13–27. <https://doi.org/10.1056/NEJMoa1614362> PMID: 28604169
2. Saklayen MG. The global epidemic of the metabolic syndrome. *Curr. Hypertens. Rep.* 2018; 20: 1–8. <https://doi.org/10.1007/s11906-018-0803-0> PMID: 29349522
3. Locke AE, Kahali B, Berndt SI, Justice AE, Pers TH, Day FR, et al. Genetic studies of body mass index yield new insights for obesity biology. *Nature* 2015; 518:197–206. <https://doi.org/10.1038/nature14177> PMID: 25673413
4. Mattson MP. An evolutionary perspective on why food overconsumption impairs cognition. *Trends Cogn. Sci.* 2019; 23: 200–212. <https://doi.org/10.1016/j.tics.2019.01.003> PMID: 30670325
5. Monda V, La Marra M, Perrella R, Caviglia G, Iavarone A, Chieffi S, et al. Obesity and brain illness: from cognitive and psychological evidences to obesity paradox. *Diabetes, Metab. Syndr. Obes. Targets Ther.* 2017; 10: 473–479. <https://doi.org/10.2147/DMSO.S148392> PMID: 29200883
6. Ugur B, Chen K, Bellen HJ. *Drosophila* tools and assays for the study of human diseases. *Dis. Model. Mech.* 2016; 9:235–244. <https://doi.org/10.1242/dmm.023762> PMID: 26935102
7. Mattila J, Hietakangas V. Regulation of carbohydrate energy metabolism in *Drosophila melanogaster*. *Genetics* 2017; 207:1231–1253. <https://doi.org/10.1534/genetics.117.199885> PMID: 29203701
8. Heier C, Kühnlein RP. Triacylglycerol metabolism in *Drosophila melanogaster*. *Genetics* 2018; 210:1163–1184. <https://doi.org/10.1534/genetics.118.301583> PMID: 30523167
9. Musselman LP, Kühnlein RP. *Drosophila* as a model to study obesity and metabolic disease. *J. Exp. Biol.* 2018; 221: jeb163881. <https://doi.org/10.1242/jeb.163881> PMID: 29514880
10. Musselman LP, Fink JL, Narzinski K, Ramachandran PV, Hathiramani SS, Cagan RL, et al. A high-sugar diet produces obesity and insulin resistance in wild-type *Drosophila*. *Dis. Model. Mech.* 2011; 4: 842–849. <https://doi.org/10.1242/dmm.007948> PMID: 21719444
11. Reed LK, Lee K, Zhang Z, Rashid L, Poe A, Hsieh B, et al. Systems genomics of metabolic phenotypes in wild-type *Drosophila melanogaster*. *Genetics* 2014; 197: 781–793. <https://doi.org/10.1534/genetics.114.163857> PMID: 24671769
12. Williams S, Dew-Budd K, Davis K, Anderson J, Bishop R, Freeman K, et al. Metabolomic and gene expression profiles exhibit modular genetic and dietary structure linking metabolic syndrome phenotypes in *Drosophila*. *G3* 2015; 5: 2817–2829. <https://doi.org/10.1534/g3.115.023564> PMID: 26530416
13. Cázarez-García D, Ramírez Loustalot-Laclette M, Markow TA, Winkler R. Lipidomic profiles of *Drosophila melanogaster* and cactophilic fly species: models of human metabolic diseases. *Integr. Biol.* 2017; 9: 885–891. <https://doi.org/10.1039/c7ib00155j> PMID: 29043354
14. Nazario-Yepiz NO, Loustalot-Laclette MR, Carpenteyro-Ponce J, Abreu-Goodger C, Markow TA. Transcriptional responses of ecologically diverse *Drosophila* species to larval diets differing in relative sugar and protein ratios. *PLoS One* 2017; 12: e0183007. <https://doi.org/10.1371/journal.pone.0183007> PMID: 28832647
15. Zhou S, Morgante F, Geisz MS, Ma J, Anholt RRH, Mackay TFC. Systems genetics of the *Drosophila* metabolome. *Genome Res.* 2020; 30: 392–405. <https://doi.org/10.1101/gr.243030.118> PMID: 31694867
16. Rajan A, Perrimon N. Of flies and men: insights on organismal metabolism from fruit flies. *BMC Biol.* 2013; 11: 1–8. <https://doi.org/10.1186/1741-7007-11-1> PMID: 23294804
17. Palm W, Sampaio JL, Brankatschk M, Carvalho M, Mahmoud A, Shevchenko A, et al. Lipoproteins in *Drosophila melanogaster*—Assembly, function, and influence on tissue lipid composition. *PLoS Genet.* 2012; 8: e1002828. <https://doi.org/10.1371/journal.pgen.1002828> PMID: 22844248
18. Gutierrez E, Wiggins D, Fielding B, Gould AP. Specialized hepatocyte-like cells regulate *Drosophila* lipid metabolism. *Nature* 2007; 445: 275–280. <https://doi.org/10.1038/nature05382> PMID: 17136098
19. Grönke S, Müller G, Hirsch J, Fellert S, Andreou A, Haase T, et al. Dual lipolytic control of body fat storage and mobilization in *Drosophila*. *PLoS Biol.* 2007; 5: 1248–1256. <https://doi.org/10.1371/journal.pbio.0050137> PMID: 17488184
20. Bharucha KN, Tarr P, Zipursky SL. A glucagon-like endocrine pathway in *Drosophila* modulates both lipid and carbohydrate homeostasis. *J. Exp. Biol.* 2008; 211: 3103–3110. <https://doi.org/10.1242/jeb.016451> PMID: 18805809

21. Patel RT, Soulages JL, Hariharasundaram B, Arrese EL. Activation of the lipid droplet controls the rate of lipolysis of triglycerides in the insect fat body. *J. Biol. Chem.* 2005; 280: 22624–22631. <https://doi.org/10.1074/jbc.M413128200> PMID: 15829485
22. Molaei M, Vandehoef C, Karpac J. NF- κ B shapes metabolic adaptation by attenuating Foxo-mediated lipolysis in *Drosophila*. *Dev. Cell* 2019; 49: 802–810. <https://doi.org/10.1016/j.devcel.2019.04.009> PMID: 31080057
23. Grönke S, Mildner A, Fellert S, Tennagels N, Petry S, Müller G, et al. Brummer lipase is an evolutionary conserved fat storage regulator in *Drosophila*. *Cell Metab.* 2005; 1: 323–330. <https://doi.org/10.1016/j.cmet.2005.04.003> PMID: 16054079
24. Fischer J, Lefèvre C, Morava E, Mussini JM, Laforêt P, Negre-Salvayre A, et al. The gene encoding adipose triglyceride lipase (*PNPLA2*) is mutated in neutral lipid storage disease with myopathy. *Nat. Genet.* 2007; 39: 28–30. <https://doi.org/10.1038/ng1951> PMID: 17187067
25. Wat LW, Chao C, Bartlett R, Buchanan JL, Millington JW, Chih HJ, et al. A role for triglyceride lipase *brummer* in the regulation of sex differences in *Drosophila* fat storage and breakdown. *PLoS Biol.* 2020; 18: 1–53. <https://doi.org/10.1371/journal.pbio.3000595> PMID: 31961851
26. Liu Z, Huang X. Lipid metabolism in *Drosophila*: development and disease. *Acta Biochim Biophys Sin* 2013; 45: 44–50. <https://doi.org/10.1093/abbs/gms105> PMID: 23257293
27. Bi J, Xiang Y, Chen H, Liu Z, Grönke S, Kühnlein RP, et al. Opposite and redundant roles of the two *Drosophila*: perilipins in lipid mobilization. *J. Cell Sci.* 2012; 125: 3568–3577. <https://doi.org/10.1242/jcs.101329> PMID: 22505614
28. Carvalho M, Sampaio JL, Palm W, Brankatschk M, Eaton S, Shevchenko A. Effects of diet and development on the *Drosophila* lipidome. *Mol. Syst. Biol.* 2012; 8: 1–17.
29. Oxenkrug G, Navrotskaya V, Vorobyova L, Summergrad P. Extension of life span of *Drosophila melanogaster* by the inhibitors of tryptophan-kynurenine metabolism. *Fly (Austin)* 2011; 5: 307–309. <https://doi.org/10.4161/fly.5.4.18414> PMID: 22041575
30. Mangge H, Summers KL, Meinitzer A, Zelzer S, Almer G, Prassl R, et al. Obesity-related dysregulation of the Tryptophan-Kynurenine metabolism: role of age and parameters of the metabolic syndrome. *Obesity* 2014; 22: 195–201. <https://doi.org/10.1002/oby.20491> PMID: 23625535
31. Harbison ST, Yamamoto AH, Fanara JJ, Norga KK, Mackay TFC. Quantitative trait loci affecting starvation resistance in *Drosophila melanogaster*. *Genetics* 2004; 166: 1807–1823. <https://doi.org/10.1534/genetics.166.4.1807> PMID: 15126400
32. Harbison ST, McCoy LJ, Mackay TFC. Genome-wide association study of sleep in *Drosophila melanogaster*. *BMC Genomics* 2013; 14: 281. <https://doi.org/10.1186/1471-2164-14-281> PMID: 23617951
33. Jaime MDLA, Hurtado J, Ramirez Loustalot-Laclette M, Oliver B, Markow T. Exploring effects of sex and diet on *Drosophila melanogaster* head gene expression. *J. Genomics* 2017; 5: 128–131. <https://doi.org/10.7150/jgen.22393> PMID: 29109800
34. Rehman N, Varghese J. Larval nutrition influences adult fat stores and starvation resistance in *Drosophila*. *PLoS One* 2021; 16: e0247175. <https://doi.org/10.1371/journal.pone.0247175> PMID: 33606785
35. Blumrich A, Vogler G, Dresen S, Diop SB, Jaeger C, Leberer S, et al. Fat-body brummer lipase determines survival and cardiac function during starvation in *Drosophila melanogaster*. *iScience* 2021; 24:102288. <https://doi.org/10.1016/j.isci.2021.102288> PMID: 33889813
36. Ogilvie RP, Patel SR. The epidemiology of sleep and obesity. *Sleep Heal.* 2017; 3: 383–388.
37. Noordam R, Bos MM, Wang H, Winkler TW, Bentley AR, Kilpeläinen TO, et al. Multi-ancestry sleep-by-SNP interaction analysis in 126,926 individuals reveals lipid loci stratified by sleep duration. *Nat. Commun.* 2019; 10: 5121. <https://doi.org/10.1038/s41467-019-12958-0> PMID: 31719535
38. Vozoris NT. Insomnia symptoms are not associated with dyslipidemia: a population-based Study. *Sleep* 2016; 39: 551–558. <https://doi.org/10.5665/sleep.5524> PMID: 26612387
39. Thompson SN. Trehalose—The insect “blood” sugar. *Adv. In Insect Phys.* 2003; 31: 205–285. [https://doi.org/10.1016/s1096-4959\(03\)00110-6](https://doi.org/10.1016/s1096-4959(03)00110-6) PMID: 12831766
40. Sayej WN, Paul R Knight Iii PR, Guo WA, Mullan B, Ohtake PJ, Davidson BA, et al. Advanced glycation end products induce obesity and hepatosteatosis in CD-1 wild-type mice. *Biomed Res. Int.* 2016; 2016: 1–12. <https://doi.org/10.1155/2016/7867852> PMID: 26942201
41. Agh F, Shidfar F. The effects of dietary advanced glycation end products (AGEs) on liver disorders in dietary interventions in liver disease: foods, nutrients, and dietary supplements (eds. Watson, R. R. & Preedy, V. R.) 213–231 (Elsevier Inc., 2019). <https://doi.org/10.1016/B978-0-12-814466-4.00018-5>
42. Pendleton RG, Rasheed A, Sardina T, Tully T, Hillman R. Effects of tyrosine hydroxylase mutants on locomotor activity in *Drosophila*: a study in functional genomics. *Behav. Genet.* 2002; 32: 89–94. <https://doi.org/10.1023/a:1015279221600> PMID: 12036114

43. Yuan Q, Joiner WJ, Sehgal A. A sleep-promoting role for the *Drosophila* serotonin receptor 1A. *Curr. Biol.* 2016; 16: 1051–1062.
44. Majeed ZR, Abdeljaber E, Soveland R, Cornwell K, Bankemper A, et al. Modulatory action by the serotonergic system: behavior and neurophysiology in *Drosophila melanogaster*. *Neural Plast.* 2016; 2016: 7291438. <https://doi.org/10.1155/2016/7291438> PMID: 26989517
45. Luo J, Becnel J, Nichols CD, Nässel DR. Insulin-producing cells in the brain of adult *Drosophila* are regulated by the serotonin 5-HT 1A receptor. *Cell. Mol. Life Sci.* 2012; 69: 471–484. <https://doi.org/10.1007/s00018-011-0789-0> PMID: 21818550
46. Nam SB, Kim K, Kim BS, Im H, Lee SH, Kim S, et al. The effect of obesity on the availabilities of dopamine and serotonin transporters. *Sci. Rep.* 2018; 8: 4924. <https://doi.org/10.1038/s41598-018-22814-8> PMID: 29563547
47. Wang G-J, Volkow ND, Logan J, Pappas NR, Wong CT, Zhu W, et al. Brain dopamine and obesity. *Lancet* 2001; 357: 354–357. [https://doi.org/10.1016/s0140-6736\(00\)03643-6](https://doi.org/10.1016/s0140-6736(00)03643-6) PMID: 11210998
48. Dietzl G, Chen D, Schnorrer F, Su K-C, Barinova Y, Fellner M, et al. A genome-wide transgenic RNAi library for conditional gene inactivation in *Drosophila*. *Nature* 2007; 448: 151–156. <https://doi.org/10.1038/nature05954> PMID: 17625558
49. Cichewicz K, Hirsh J. ShinyR-DAM: A program analyzing *Drosophila* activity, sleep and circadian rhythms. *Commun. Biol.* 2018; 1: 1–5. <https://doi.org/10.1038/s42003-017-0002-6> PMID: 29809203
50. Shaw PJ, Cirelli C, Greenspan RJ, Tononi G. Correlates of sleep and waking in *Drosophila melanogaster*. *Science* 2000; 287:1834–1837. <https://doi.org/10.1126/science.287.5459.1834> PMID: 10710313
51. Franz M, Lopes CT, Huck G, Dong Y, Sumer O, Bader GD, Cytoscape.js: A graph theory library for visualisation and analysis. *Bioinformatics* 2016; 32: 309–311. <https://doi.org/10.1093/bioinformatics/btv557> PMID: 26415722
52. Bostock M, Ogievetsky V, Heer J. D3: Data-Driven Documents. *IEEE Trans. Vis. Comput. Graph.* 2011; 17: 2301–2309. <https://doi.org/10.1109/TVCG.2011.185> PMID: 22034350